Design of Beamforming conformal antenna array based on Partially Reflecting Surfaces

Vivek Kumar*, Christophe Craeye*
*ICTEAM Institute, UCLouvain, Louvain-la-Neuve, Belgium
vivek.kumar@uclouvain.be, christophe.craeye@uclouvain.be

***Abstract*—A multi-faceted array using Partially Reflecting Surfaces (PRSs) for satellite communication is proposed. The beamforming algorithm is formulated using phase correction as well as amplitude weighting proportional to the level of embedded patterns in the direction of the scan. The pattern is effectively scanned within the field of view defined by the angular width of a facet. A fluctuation in maximum gain of less than 1 dB has been achieved, with a sidelobe level of -8.17 dB, though further research is needed to improve the sidelobe level.**

***Index Terms*—Antennas, Partially Reflecting Surface, Beamfoming, Radiation pattern, Multifaceted array, Satellite Communication.**

I. Introduction

The final application of this work is to download data from a satellite while it is still very close to the horizon, which requires an antenna with sufficient effective area, a high beamformed pattern, and low sidelobe level. When a satellite approaches the horizon, its distance to the ground station is at its greatest. Besides, the antennas placed on the lower side of the array may not offer a sufficient effective area. From this point, the need for a conformal array arises (see Fig. 1). Furthermore, beamforming capabilities enable the system to dynamically direct and combine signals from different parts of the array, focusing energy in the desired direction. This boosts the antenna's gain and effective area, allowing for robust and dependable communication even when the satellite is low on the horizon.

Regarding the gain enhancement, Partially Reflective Surface (PRS) antennas have drawn significant attention due to their compact design and simple way of achieving high gain [1]. The fundamental construction of a PRS is relatively simple. A source antenna, frequently a microstrip patch antenna feeds the Fabry Perot Cavity (FPC) formed by the antenna's ground plane and the PRS element kept at approximately half of a wavelength ($\lambda/2$) [2]. The electromagnetic waves (EM) arising from the source involve many reflections within the cavity, and a certain portion of their energy is transmitted through the PRS upon every reflection. The span between the ground plane and the PRS is normally opted so that electromagnetic waves transmitted across the PRS get involved constructively at broadside direction at the operating frequency.

In reference [3], the Fabry Perot Cavity (FPC) antenna is designed for high data rate CubeSat Communication, which gives left-hand circular polarization (LHCP) with a realized gain of 15.1 dBi at an operating frequency of 8.7 GHz. It has a gain fluctuation of bandwidth (BW) of 6%. In [4], the authors presented a high-gain broadband Fabry-Perot type antenna based on a three-layer partially reflective surfaces (PRSs), which yields around 20 dBi gain and bandwidth of approximately 15% at an operating frequency of 14.5 GHz.

In the literature, many methods have been used to perform beamforming. In [5], the authors proposed a conformal phased array with beamforming for satellite communication based on a truncated Singular Value Decomposition. An effective computation method for phased arrays with large scanning coverage extension is the pattern reconfigurable method [6]. In [7], a reconfigurable design based on a coupled-mode patch is explained. Although the above-named techniques can implement beamforming, they have some drawbacks, such as complex nonplanar structure, efficiency, and gain fluctuation.

The remainder of this paper is organized as follows. The design of the unit cell high-gain antenna is described in Section II. The mathematical analysis and implementation of beamforming is explained in Section III. Conclusions are drawn in Section IV.

II. Unit Antenna Design

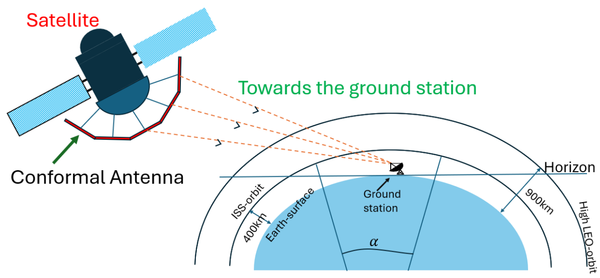

Fig. 1. Basic communication arrangement between Ground Station and Satellite

The basic satellite communication configuration is shown in Fig. 1. Maximising signal strength and maintaining a strong link with ground stations is critical throughout the satellite's trajectory. When the satellite is near the horizon, it faces significant challenges due to increased free-space path loss and atmospheric attenuation because this is the distance to the ground station that is largest. To address this, faceted antenna conformal arrays offer an effective solution that combines both structural and signal processing advantages with few active components. This increases the antenna's gain and effective area, ensuring strong and reliable communication. This section explains the design of the unit antennas for conformal arrays.

The schematics of the unit PRS antenna is shown in Fig. 2 [9]. A rectangular patch antenna is kept at a height, h below the PRS, the patch serves as a radiating source element. The proposed antenna is designed and simulated using commercial frequency domain solver of CST Microwave Studio [8]. The design operates at a selected frequency, f of 23 GHz. The dimension of the PRS structure shown in Fig. 3(a) is

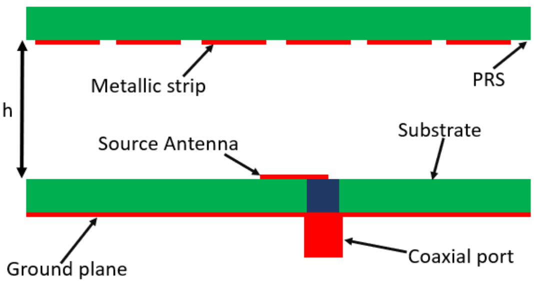

Fig. 2. Schematic of the unit antenna structure : Side view

32.395 mm × 29.85 mm × 0.8 mm (i.e., $2.48 \times 2.28 \times 0.06\lambda^3$). The substrate used for PRS and antenna structure is Rogers RT5880, which has a low dielectric constant ($\epsilon_r = 2.2$) and low dielectric loss (tanδ = 0.0009). The PRS structure contains 15 × 15 metallic patches with dimensions of 1.85 mm × 1.85 mm × 0.035 mm (i.e., $0.14 \times 0.14 \times 0.0026\lambda^3$). The source patch antenna shown in Fig. 3(b) has dimensions of 2 mm × 3 mm × 0.035 mm (i.e., $0.153 \times 0.23 \times 0.0026\lambda^3$) feed by a coaxial probe.

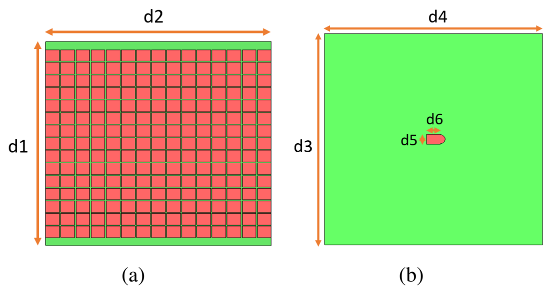

Fig. 3. (a) PRS structure and (b) Patch structure

Fig. 4 represents the radiation pattern of 2-D farfield of the proposed antenna with and without PRS in E- and H- planes, respectively. As expected, when the PRS is added, the radiation pattern becomes more focused. Fig. 5 shows the gain plot of the proposed antenna with and without the PRS as a function of frequency, and a significant gain enhancement is observed.

III. Formulation and Implementation of Beamforming

In this work, the antenna elements are organized in conformal array with an angle α between consecutive facets, at a distance of R from the center. The 2D view of the antenna array

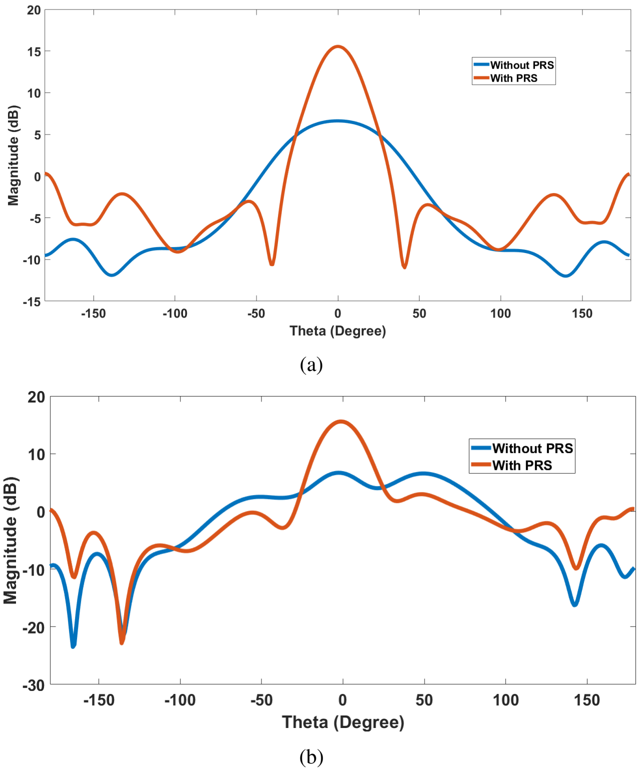

Fig. 4. (a) E plane Pattern and (b) H Plane Pattern of the proposed structure with and without PRS, at 23 GHz.

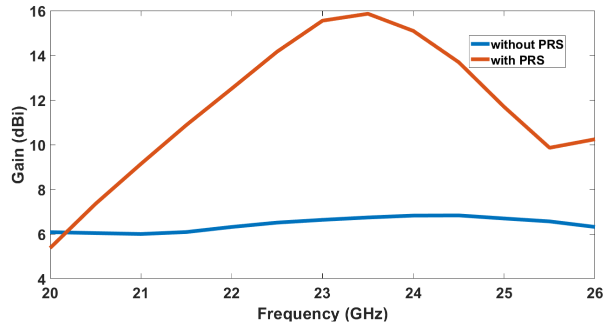

Fig. 5. Gain at broadside of one facet of the proposed antenna with and without PRS.

is shown in Fig. 6. Each facet is designed to be manufactured individually and assembled by screwing them together. The total number of facets dictates the necessary beam coverage, and the number of adjacent facets determines the angular field of view. This section explains the beamforming techniques applied to cylindrical array antenna using the radiation pattern obtained in the previous section. More precisely, coupling with neighboring facets will be included, and the embedded element pattern (EEP) concept is used.

Suppose there is a group of N antennas, and let F_i represent the field radiated by the i_{th} element (one PRS-based facet in this case) in the presence of the other antennas,

$$\vec{F_i} = |F_i(\theta)|\, e^{j\varphi_i(\theta)} \quad (1)$$

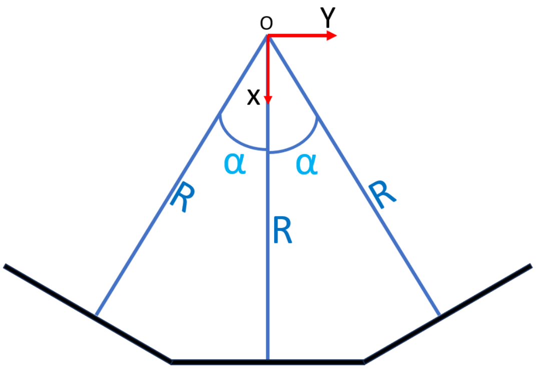

Fig. 6. 2D view of antenna array

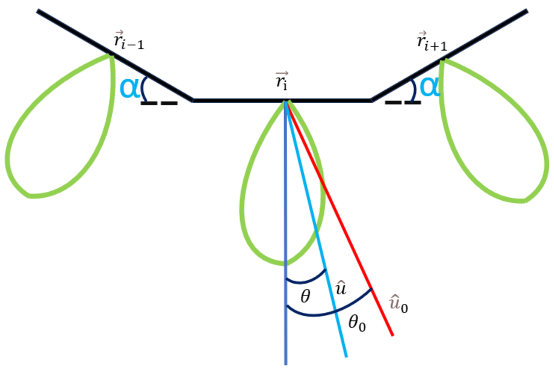

Fig. 7. Unit vector direction

The complex values of F_i are obtained with the help of the commercial software CST Microwave Studio. The structure is either closed (α integer fraction of 2π) or has a large number of facets such that the embedded element patterns (EEPs) of each facet can be supposed identical.

The field in the direction θ from the i_{th} element of the array shown in Fig. 7 is given by

$$\vec{F}_i(\theta) = |F_i(\theta)|\, e^{j\varphi_i(\theta)} e^{-jk\hat{u}\cdot\vec{r}_i} \tag{2}$$

where $k = 2\pi/\lambda$ is the free-space wavenumber with λ being the wavelength of the signal, $\vec{r}_i$ is the reference point for phase on i_{th} antenna, taken here at the intersection between connector and ground plane, and $\hat{u}$ is the direction of observation. Due to rotational symmetry of the structure,

$$\vec{F}_i(\theta) = \vec{F}_0(\theta - i\alpha) \tag{3}$$

where $\vec{F}_0$ is the embedded pattern associated with the facet that is pointing towards nadir. The radiation pattern in the α angle from the i_{th} facet antenna is given by (3). So, using equations (2) and (3),

$$\vec{F}_i(\theta) = |F_0(\theta - i\alpha)|\, e^{j\varphi((\theta - i\alpha))} e^{-jk\hat{u}\cdot\vec{r}_i} \tag{4}$$

where the last factor accounts for differences in the distances of propagation. Then, the beamformer output is

$$\vec{P}(\theta) = \sum_{i=1}^{N} |F_0(\theta - i\alpha)|\, e^{j\varphi(\theta - i\alpha)} e^{-jk\hat{u}\cdot\vec{r}_i} w_i \tag{5}$$

where $w_i = e^{j\psi_i}$ is the beamforming weight which is chosen to steer the beam in direction θ_0. $\vec{P}(\theta)$ is the pattern of the array, which is the sum of contributions from each facet, with a given weight w_i. To maximize the output in direction θ_0, the phase of each term in (5) should be the same. So,

$$\psi_i = k\hat{u}_0 \cdot \vec{r}_i - \varphi(\theta_0 - i\alpha) \tag{6}$$

Using equations (6) and (5), the overall beamformer output for scanning in the direction θ_0 when the beam is steered into direction θ_0 is

$$P(\theta) = \sum_{i=1}^{N} \gamma_i\, |F_0(\theta - i\alpha)|\, e^{j\varphi(\theta - i\alpha)} e^{-jk(\hat{u} - \hat{u}_0)\cdot\vec{r}_i} e^{j\varphi(\theta_0 - i\alpha)} \tag{7}$$

where $\gamma_i = |F_0(\theta_0 - i\alpha)|$ is the magnitude of the i_{th} pattern in the desired direction θ_0. This weighting has been added in order to scale the contribution of a given facet proportionally to its level in the direction of the scan. For instance, if a facet does not send significant power in the direction of scan it should not contribute significantly to the beamforming operation.

In this simulated work, three facets are used, with an angular rotation of $\alpha = 20°$ between consecutive facets. Among the three facets, the middle one is excited to obtain an embedded element pattern, $\vec{F}_0$. In this way, the effects of coupling with neighboring facets are included. Using that pattern, the obtained beam is steered as explained above from $-\alpha/2$ to $\alpha/2$ around broadside, i.e., $-10°$ to $10°$, in this case.

A maximum gain fluctuation of 0.26 dB is observed among the beams of chosen directions. The side lobe level (SLL) is 8.17 dB below the main beam, which is not ideal. Further research is needed to improve this aspect. Although the array is not planar, the high sidelobes can be explained as remainders of grating lobes, which are not fully suppressed by the narrow EEP [10]. However, the main shape is not highly influenced by the steering. Figure 8 shows the three beams towards $-10°$, $0°$ and $10°$.

Consequently, the proposed antenna can achieve continuous beam-scanning over an angular range of $20°$. For scanning further away, beamforming with the next set of facets is carried out.

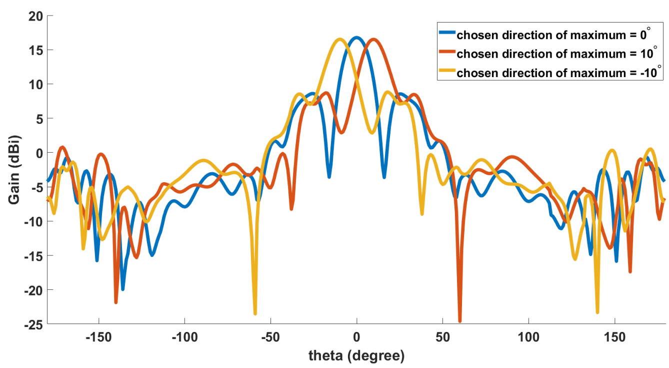

Fig. 8. Steered beams in the chosen direction.

Furthermore, a comparative graph is plotted for the Embedded Element Pattern and the beamformed pattern when the chosen direction of maximum is $0°$; see Fig. 9. The beamformed pattern has been normalised by $\sum_i |\gamma_i|^2$ in order to compare patterns with same input power.

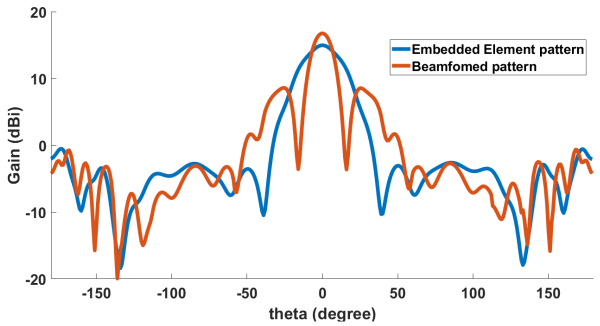

Fig. 9. Comparison between E−plane Embedded Element Pattern and Beamformed pattern in the chosen direction of maximum = $0°$.

TABLE I
COMPARISON BETWEEN THIS WORK AND SEVERAL OTHER ANTENNAS

Ref.	Size	Gain (dBi)	Gain drop	scan-angle
[11]	$1.9\lambda\times1.9\lambda$	Directivity 14.8 dBi	NA	$\pm7°$
[12]	$3.1\lambda\times3.1\lambda$	$11.8-14.3$ dBi	2.5 dBi	$\pm15°$
[13]	$2.75\lambda\times2.75\lambda$	$11.5-12.3$ dBi	0.8 dBi	$\pm18°$
This work	$\mathbf{2.48\lambda\times2.2\lambda}$	**16.76 dBi**	**0.26 dBi**	$\pm\mathbf{10°}$

Table I shows a comparison of the unit size, radiation parameters, and scan-angle of the proposed simulated beamforming antenna to various reported hardware designs. The suggested simulated antenna has a high gain and a decent steering angle with minimal gain drop. Nevertheless, the hardware design accounts for real-world constraints, such as material loss, manufacturing tolerance, and lab environment effects.

IV. CONCLUSION

A high-gain broadband multi-faceted array based on the optimized PRS has been designed using CST software for satellite applications. The beamforming is based on generating the radiation pattern of the antenna array by adding in-phase the signals of a few consecutive facets in the required direction, with magnitudes proportional to the level of respective embedded patterns in the same direction. Since the array is conformal, grating lobes are only partially present.

Using this method, the pattern has been effectively scanned from $-10°$ to $10°$, i.e., the range imposed by the angle between consecutive facets, with less than 1 dB fluctuation in the maximum gain. The -8.17 dB sidelobe level achieved so far calls for further research, for instance, by producing sharper embedded element patterns through the exploitation of coupling between consecutive facets.

ACKNOWLEDGEMENT

This research is part of the Space4ReLaunch project, which is supported by the SPW Economie Emploi Recherche of the Walloon Region, under grant agreement no. 2210181.

REFERENCES

[1] L. Leger, T. Monediere, and B. Jecko, “Enhancement of gain and radiation bandwidth for a planar 1-D EBG antenna,” IEEE Microw. Wireless Compon. Lett., vol. 15, no. 9, pp. 573–575, Sep. 2005.
[2] G. Trentini, “Partially reflecting sheet arrays,” IRE Trans. Antennas Propag., vol. 4, no. 4, pp. 666–671, Oct. 1956.
[3] R. De, M. P. Abegaonkar and A. Basu, ”X-band superstrate antenna for high data rate cubesat communication,” 2023 IEEE International Symposium on Antennas and Propagation and USNC-URSI Radio Science Meeting (USNC-URSI), Portland, OR, USA, 2023.
[4] K. Konstantinidis, A. P. Feresidis, and P. S. Hall, “Multilayer partially reflective surfaces for broadband Fabry–Pérot cavity antennas,” IEEE Trans. Antennas Propag., vol. 62, no. 7, pp. 3474–3481, Jul. 2014.
[5] H. Schippers et al., “Conformal phased array with beam forming for airborne satellite communication,” in Proc. Int. ITG Workshop Smart Antennas, Feb. 2008, pp. 343–350.
[6] G. Yang, J. Li, S. G. Zhou, and Y. Qi, “A wide-angle E-plane scanning linear array antenna with wide beam elements,” IEEE Antennas Wireless Propag. Lett., vol. 16, pp. 2923–2926, 2017.
[7] Haozhan Tian, Li Jun Jiang, and Tatsuo Itoh, ”A compact single-element pattern reconfigurable antenna with wide-angle scanning tuned by a single varactor,” Progress In Electromag. Res. C, vol. 92, 137-150, 2019.
[8] https://www.3ds.com/products/simulia/cst-studio-suite
[9] A. P. Feresidis, G. Goussetis, S. Wang, and J. C. Vardaxoglou, “Artificial magnetic conductor surfaces and their application to low-profile high-gain planar antennas,” IEEE Trans. Antennas Propag., vol. 53, no. 1, pp. 209–215, Jan. 2005.
[10] J. Dessy, M. Bodehou, J. Cavillot and C. Craeye, ”Sparse-Array Metasurface for Beam Scanning,” IEEE Trans. on Antennas and Propag., vol. 72, no. 10, pp. 8088-8093, Oct. 2024.
[11] A. Ourir, S. N. Burokur and A. De Lustrac, ”Electronic beam steering of an active metamaterial-based directive subwavelength cavity,” 2nd Euro. Conf. Antennas and Propag., EuCAP 2007, Edinburgh, 2007, pp. 1-4.
[12] L.-Y. Ji, Y. J. Guo, P.-Y. Qin, S.-X. Gong, and R. Mittra, “A reconfigurable partially reflective surface (PRS) antenna for beam steering,” IEEE Trans. Antennas Propag., vol. 63, no. 6, pp. 2387–2395, Jun. 2015.
[13] L. -Y. Ji, P. -Y. Qin, J. -Y. Li and L. -X. Zhang, “1-D Electronic beam-steering partially reflective surface antenna,” IEEE Access, vol. 7, pp.115959-115965, 2019.